On the Large Eddy Simulation of Scalar Transport with Prandtl Number up to 10 Using Dynamic Mixed Model

Yang Na*

CAESIT, Department of Mechanical Engineering, College of Engineering, Konkuk University, Seoul 143-701, Korea

The dynamic mixed model (DMM) combined with a box filter of Zang et. al. (1993) has been generalized for passive scalar transport and applied to large eddy simulation of turbulent channel flows with Prandtl number up to 10. Results from a priori test showed that DMM is capable of predicting both subgrid-scale (SGS) scalar flux and dissipation rather accurately for the Prandtl numbers considered. This would suggest that the favorable feature of DMM, originally developed for the velocity field, works equally well for scalar transport problem. The validity of the DMM has also been tested a posteriori. The results of the large eddy simulation showed that DMM is superior to the dynamic Smagorinsky model in the prediction of scalar field and the model performance of DMM depends to a lesser degree on the ratio of test to grid filter widths, unlike in the a priori test.

Key Words : Temperature Field, Prandtl Number, Subgrid-scale Diffusivity, Large Eddy Simulation

Nomenclature

C_S, C_T : Model coefficients
h : Half channel height
L_x, L_z : Domain size in the streamwise and spanwise directions, respectively
q_j : Residual scalar flux vector
p : Pressure
Pr : Molecular Prandtl number
$\mathrm{Pr}_{t,SGS}$: SGS turbulent Prandtl number
Re_h : Reynolds number based on bulk velocity and half channel height, $\frac{U_b h}{\nu}$
Re_τ : Reynolds number based on friction velocity and half channel height, $\frac{u_\tau h}{\nu}$
S_{ij} : Strain rate tensor
t : Time
T : Passive scalar
$\overline{T}$: Mean passive scalar
T_{rms} : Passive scalar intensities
T_w : Constant wall temperature (passive scalar) at upper wall
T_τ : Friction temperature, $\frac{q_w}{\rho C_p u_\tau}$
u, v, w : Velocity component in x, y, z directions, respectively
u_τ : Friction velocity at inlet of the domain
U_b : Bulk velocity
x, y, z : Cartesian coordinate in the streamwise, wall-normal and spanwise directions
Δ : Filter width
α : Ratio of the filter width
α_t : Turbulent diffusivity
ε_τ, ε_q : Subgrid-scale dissipation and scalar dissipation
ν_t : Turbulent viscosity
τ_{ij} : Residual stress tensor

Superscripts

$-$, $\sim$: Grid, test filter
$+$: Wall variables

* **E-mail** : yangna@konkuk.ac.kr
TEL : +82-2-450-3467; **FAX** : +82-2-447-5886
CAESIT, Department of Mechanical Engineering, College of Engineering, Konkuk University, Seoul 143-701, Korea. (Manuscript **Received** October 15, 2004; **Revised** January 20, 2005)

Operators

$\langle\ \rangle$: Time-averaged quantities

1. Introduction

Most of engineering applications in complex geometries involving flows require accurate prediction methods for turbulent flows. Direct numerical simulation (DNS) is restricted to a relatively low Reynolds number because of the need to resolve all the spatial scales of turbulence. Nearly all of the computational cost in DNS is expended on the smallest motions, which have a dissipative nature, and the resulting high cost makes DNS less attractive as an engineering tool at present. In large eddy simulation (LES), on the other hand, only the dynamics of the larger-scale motions (which are not universal) are computed explicitly while the effects of small scales or subgrid-scales (which have, to some extent, a universal character) are represented by simple models. Thus, the critical issue in LES is to accurately capture the effects of the unresolved subgrid-scale (SGS) motions using simple and universal models.

The most widely used Smagorinsky model has some notable drawbacks as noted by Zang et al.(1993): (1) it requires an input of a model coefficient which is flow-dependent; (2) it predicts incorrect asymptomatic behavior in the vicinity of a wall; (3) it does not allow energy backscatter from small scales to large scales; and (4) it assumes that principal axes of the SGS stress tensor are aligned with those of the resolved strain rate tensor.

Extensive effort has been made in the development of LES methodologies in order to overcome some of the aforementioned drawbacks of the original Smagorinsky model. For example, in the 'pioneering' dynamic Smagorinsky model (DSM) proposed by Germano et al.(1991), the model coefficient is calculated dynamically during computation using information from the resolved scales. Many of the earlier studies have shown that DSM can be successfully applied to LES of transitional and turbulent channel flows. In spite of its many desirable features and its success, the DSM still has several aspects that need to be improved, prompting subsequent development of the dynamic mixed model (DMM) of Zang et al. (1993). They modified the dynamic eddy viscosity model by employing the scale similarity model of Bardina et al.(1983) as the base model, in which the Leonard term is computed explicitly while the cross term is modeled by the scale-similarity assumption. DMM retains the desirable features of the DSM, but it does not require the SGS stress tensor and the strain rate tensor to be aligned. Furthermore, it could successfully reduce the excessive backscatter represented by the model coefficient by calculating the modified Leonard term explicitly while modeling only the remaining residual stress term. Zang et al.(1993) also successfully applied DMM to the LES of flows in a lid-driven cavity, using a finite volume approach with a box filter employed in physical space.

This brief literature indicates that significant development has been made to the LES modeling for the prediction of a turbulent velocity field, but much less effort has been done in the calculation of passive scalar transport in spite of its practical importance. The difficulty of investigating passive scalar transport is possibly due to the urgent need for improving the accuracy of LES models for the velocity field, and also to the fact that errors associated with LES models embedded in a velocity field reduces the accuracy in the prediction of passive scalar. Consequently, the transport of passive scalar from an LES point of view is still poorly understood, and this fact is reflected in the difficulty of predicting the passive scalar field with satisfactory accuracy using current LES models.

The present work is mainly motivated by the need for information on the performance of existing LES models, specifically DMM, for passive scalar transport with moderate Prandtl number (up to 10 at present). DMM was chosen here for the following two reasons: (1) From the perspective of large eddy simulation of engineering flows, computations based on finite difference formulations are certainly of great interest. Thus, DMM with finite difference formulations, which most conveniently use filters in physical space,

were considered and tested for turbulent channel flows; (2) DMM has been successfully applied in many turbulent flows (Kang, 2000).

Previous work of Na (2004) showed that the performance of DSM degrades rapidly as the Prandtl number increases and this fact led to the present work of pursuing a better LES model for passive scalar from an engineering point of view. Even though Calmet and Magnaudet (1997) showed the success for the high Schmidt number mass transfer problem with DMM, the detailed information about the performance of DMM for the passive scalar was not investigated and this motivates the present work.

In the next section, the procedure of extending the original dynamic mixed model of Zang et al. (1993) to passive scalar transport is summarized and its characteristics are discussed in the case of turbulent channel flow. The model was tested both a priori using direct numerical simulation data and a posteriori in an actual LES.

2. Numerical Methodology

2.1 Mathematical Formulation for LES

For incompressible flows, the filtered governing equations (written in a conservative form) for the LES of a passive scalar are

$$\frac{\partial \overline{u}_i}{\partial x_i}=0 \tag{1}$$

$$\frac{\partial \overline{u}_i}{\partial t}+\frac{\partial}{\partial x_j}(\overline{u}_i\overline{u}_j) =-\frac{1}{\rho}\frac{\partial \overline{p}}{\partial x_i}+\frac{\partial}{\partial x_j}(2\nu \overline{S}_{ij}-\tau_{ij}) \tag{2}$$

$$\frac{\partial \overline{T}}{\partial t}+\frac{\partial}{\partial x_j}(\overline{T}\overline{u}_j)=\frac{\partial}{\partial x_j}\left(\alpha\frac{\partial \overline{T}}{\partial x_j}-q_j\right) \tag{3}$$

where the overbar denotes the grid-filtering operation. The effect of the unresolved subgrid scales is represented by the following residual stress tensor τ_{ij} and residual scalar flux vector q_j.

$$\tau_{ij}=\overline{u_iu_j}-\overline{u}_i\overline{u}_j \tag{4}$$

$$q_j=\overline{Tu}_j-\overline{T}\,\overline{u}_j \tag{5}$$

All the terms in equations (1)-(3) are resolved except τ_{ij} and q_j which should be obtained from the models.

We employed the dynamic mixed model of Zang et al. (1993) in which the anisotropic part of the residual stress is expressed as

$$\tau_{ij}-\frac{\delta_{ij}}{3}\tau_{kk}=-2\nu_t\overline{S}_{ij}+\left(L^m_{ij}-\frac{\delta_{ij}}{3}L^m_{kk}\right) \tag{6}$$

$$\nu_t=C_S\overline{\Delta^2 S} \tag{7}$$

where

$$L^m_{ij}=\overline{\overline{u}_i\overline{u}_j}-\overline{\overline{u}}_i\overline{\overline{u}}_j \tag{8}$$

$$C_S=\frac{1}{2\overline{\Delta}^2}\frac{M_{ij}(L_{ij}-H_{ij})}{M_{kl}M_{kl}} \tag{9}$$

$$M_{ij}=[\widetilde{\overline{S}\overline{S}}_{ij}-(\widetilde{\overline{\Delta}}/\overline{\Delta})^2\widetilde{\overline{S}}\,\widetilde{\overline{S}}_{ij}] \tag{10}$$

$$L_{ij}=\widetilde{\overline{u}_i\overline{u}_j}-\widetilde{\overline{u}}_i\widetilde{\overline{u}}_j \tag{11}$$

$$H_{ij}=\widetilde{\overline{u}_i\overline{u}_j}-\widetilde{\overline{u}}_i\widetilde{\overline{u}}_j \tag{12}$$

A test-scale filter represented by a tilde was introduced here to utilize the information between the grid- and test-scale filters to determine the characteristics of subgrid scale (SGS) motion. The computed C_S is substituted into equations (6)-(7) to obtain eddy viscosity and residual stress.

In DMM, the procedure for calculating τ_{ij} can be generalized to develop an analogous model for the residual scalar flux q_j as follows:

$$q_j=-\alpha_t\frac{\partial \overline{T}}{\partial x_j}+F^m_j \tag{13}$$

$$\alpha_t=C_T\overline{\Delta^2 S} \tag{14}$$

where

$$F^m_j=\overline{\overline{T}\,\overline{u}_j}-\overline{\overline{T}}\,\overline{\overline{u}}_j \tag{158}$$

$$C_T=\frac{1}{2\overline{\Delta}^2}\frac{(F_k-G_k)H_k}{H_kH_k} \tag{16}$$

$$F_k=[\widetilde{\overline{T}\overline{u}}_k-\widetilde{\overline{T}}\,\widetilde{\overline{u}}_k \tag{17}$$

$$G_k=\widetilde{\overline{T}\overline{u}}_k-\widetilde{\overline{T}}\,\widetilde{\overline{u}}_k \tag{11}$$

$$H_k=\overline{S}\frac{\partial \widetilde{\overline{T}}}{\partial x_k}-(\widetilde{\overline{\Delta}}/\overline{\Delta})^2\widetilde{\overline{S}}\frac{\partial \widetilde{\overline{T}}}{\partial x_k} \tag{19}$$

In order to discretize the grid-scale and the test-scale filters, a box filter in physical space using Simpson's rule was employed. After the model coefficients C_G and C_T are computed through the least-squares approach (Lilly, 1992), they are averaged locally in space within the test-filtering volume as suggested by Zang et al. (1993). Also, if the total viscosity $(\nu+\nu_t)$ or diffusivity $(\alpha+\alpha_t)$

becomes negative, they are set to zero to guarantee numerical stability.

2.2 Boundary conditions

The streamwise extent of the computational domain is $L_x=13h$ and the spanwise extent is $L_z=6.5h$, where h is the half-channel height. In terms of wall units (based on friction velocity), the domain size is approximately equivalent to 1900 in streamwise, 300 in wall-normal, and 950 in the spanwise directions. The Reynolds number based on friction velocity and half-channel height, Re_τ was set to 150 while the Prandtl number, Pr, varies from 1 to 10. The present code was originally written for the simulation of spatially evolving turbulent flows and thus, requires inflow/outflow conditions. In order to provide a physically realistic turbulence to the inlet of the domain, the required velocity and temperature of the plane located at about $x/h=11$ (equivalent to approximately 1600 wall units from the inlet) were fed into the inlet plane continuously. This way of generating inflow turbulence is, in effect, equivalent to imposing a periodic boundary condition in the streamwise direction, which is frequently adopted in spectral method.

No-slip boundary condition was used along the walls. The bottom wall was cooled ($-T_w$) and the top wall was heated (T_w) at the same rate so that both walls were maintained at constant temperature. The flow was assumed to be homogeneous in the spanwise direction, justifying the use of periodic boundary conditions in that direction. A convective boundary condition, which is believed to allow turbulent structures to leave the domain smoothly, was used for the outflow boundary condition.

The governing equations (1)-(3) were integrated in time using a semi-implicit scheme. A low-storage three-substep, third order Runge-Kutta scheme was used for treating convective terms explicitly. On the other hand, a second order Crank-Nicolson scheme was used for treating viscous terms semi-implicitly (Na, 1994). All the spatial derivatives were approximated with second order central differencing scheme, except for the convective term in the equation (3). The central differencing scheme applied to the convective term in the passive-scalar equation, combined with the inflow-outflow boundary condition, is known to lead to numerical instability. Thus, a widely used QUICK scheme (Leonard, 1979) was employed as a remedy for the present work.

2.3 A priori test using DNS

An a priori test on the DMM was carried out to determine the accuracy with which the model predicts the SGS scalar flux and dissipation. Tests were performed using DNS data generated with 129^3 meshes for the turbulent channel with the same flow configurations as described in section 2.2 for Pr=1, 3 and $129\times193\times129$ meshes for Pr=10.

Grid spacings were uniform in both streamwise and spanwise directions. Based on friction velocity, the grid spacing in the streamwise direction was approximately 15.1 in wall units. In the wall-normal direction, the resolution varies with the Prandtl number. For Pr=1 and 3, the minimum grid spacing was 0.022 at the wall, whereas the maximum grid spacing was 3.7 in the middle of the channel in wall unit. For Pr=10, the minimum and maximum spacing were 0.010 at the wall and 2.5 in the middle of the channel in wall unit, respectively. The uniform grid spacing in the spanwise direction was 7.6 in terms of wall units. The adequacy of the grid resolution of the present DNS for the velocity field (129^3 meshes) obtained with finite difference scheme was assessed by comparing the 1st and 2nd order statistics of the velocity with those obtained with the pseudo-spectral method by Na et al.(1999) (Figure 1). Since the results of Na et al.(1999) were obtained also with the 129^3 meshes for $Re_\tau=150$, any difference seen in the results can be attributed to the difference in ability of resolving the high wave-number motion (or equivalently, small-scale motion) between the spectral and the finite difference methods. But the positive agreements for all the quantities shown in Figure 1 indicate that the choice of the present resolution is good enough at the Reynolds number considered in the present work.

All the filtering operations were performed in physical space using a box filter with Simpson's rule. The exact values of SGS scalar flux q_j, and SGS scalar dissipation, $\varepsilon_q=q_j\frac{\partial T}{\partial x_j}$ were directly calculated by filtering the DNS data, whereas the results of an a priori test were obtained by solving the equations (6) and (13) using the filtered DNS field. The width of the grid filter is given as $\overline{\Delta}_x=2\Delta_x$, $\overline{\Delta}_z=2\Delta_z$, and the length scale of the test filter is twice that of the grid filter, resulting in a ratio of the test-scale to the grid-scale of 2 in the streamwise and spanwise directions, respectively. No explicit filtering was applied in the wall-normal directions.

The only adjustable parameter in the DMM is the ratio of test to grid filter width, $\alpha=\widetilde{\overline{\Delta}}/\overline{\Delta}$. There is some ambiguity in defining the effective filter width on anisotropic grids, and when explicit filtering is not performed in all directions as in the present work. Two commonly used definitions of the effective filter width are:

$$\overline{\Delta}^3=\overline{\Delta}_x\overline{\Delta}_y\overline{\Delta}_z,\quad \widetilde{\overline{\Delta}}^3=\widetilde{\overline{\Delta}}_x\widetilde{\overline{\Delta}}_y\widetilde{\overline{\Delta}}_z \tag{20}$$

and

$$\overline{\Delta}^2=\overline{\Delta}_x^2+\overline{\Delta}_y^2+\overline{\Delta}_z^2,\quad \widetilde{\overline{\Delta}}^2=\widetilde{\overline{\Delta}}_x^2+\widetilde{\overline{\Delta}}_y^2+\widetilde{\overline{\Delta}}_z^2 \tag{21}$$

Since explicit filtering was not performed in the direction normal to the wall, $\overline{\Delta}_y=\widetilde{\overline{\Delta}}_y$ and the equation (20) reduces to $\alpha=2^{2/3}$. If one were to determine the effective filter width by only considering the filtered directions, one would get $\alpha=2$ instead of $2^{2/3}$. The value of $\alpha=2$ is known to be the optimal choice in the simulation of a turbulent channel flow using a sharp cutoff filter (Germano et al., 1991), but optimal value is likely to depend on the types of grid and test filters used. A larger value of would result in a larger magnitude of M_{ij} and H_k and thus, lower values of eddy viscosity and diffusivity. The sensitivity of the numerical results to the choice of α was examined for two different values of α (2 and $2^{2/3}$) and the results will be addressed later.

All the results from the a priori test were obtained by averaging the flow field in time for about 150 ν/u_τ^2. This period of time was shown to be sufficiently long enough to obtain smooth SGS statistics.

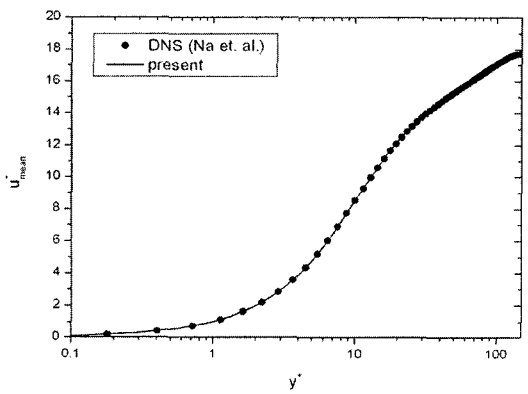

(a) Mean streamwise velocity

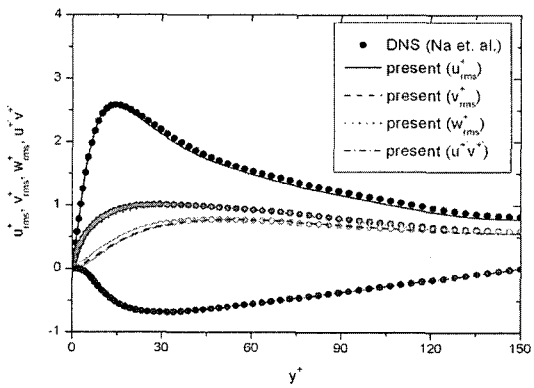

(b) Turbulence intensities

Fig. 1 Comparison of velocity statistics

2.4 LES with DMM

In order to investigate the performance of DMM applied in passive scalar, it was also tested a posteriori by conducting an LES with DMM. As in the a priori test performed on DNS data, a box filter was used for both grid and test filters in streamwise and spanwise directions, but no explicit filtering was done in the normal direction. The length scale of the grid filter is equal to the grid size, and the length scale of the test filter is twice that, resulting in a ratio of the test-scale to the grid-scale of 2 in both streamwise and spanwise directions. A grid of $65\times65\times65$ was used for all the Prandtl numbers considered (Pr=1, 3 and 10) and all the statistics were averaged over a period of 150 ν/u_τ^2.

The effect of the grid resolution for LES with DMM was assessed by examining the mean and

rms temperatures (or passive scalar) obtained using three different resolutions for the highest Prandtl number case (Pr=10) considered in the present work in Figure 2. It is well known that LES with DMM tends to result in a higher prediction of mean and rms velocities in wall units than those obtained from filtered DNS. Figure 2 shows that a similar behavior was also noted for temperature (or passive scalar) and the result improves consistently as the resolution gets better, but the degree of improvement decreases as the resolution increases. This result can provide some insight into the issue of truncation errors in the present finite difference method. Caution must be taken when numerical simulations are conducted with low-order finite difference approximation, because numerical errors (both aliasing and truncation errors) can deteriorate the subgrid-scale terms. Even though it is difficult to quantify errors in the general nonlinear turbulent flows, at least a consistent reduction of errors as resolution increases was established in Figure 2. This result would suggest that truncation errors do not significantly pollute the SGS terms, and that truncation errors can be controlled by choosing higher resolutions. From Figure 2, it is believed that the results obtained with grids are sufficiently good enough for the purpose of evaluating the performance of DMM for passive scalar at the Prandtl number considered.

3. Results

3.1 A priori test

Figures 3~5 compare the subgrid-scale scalar

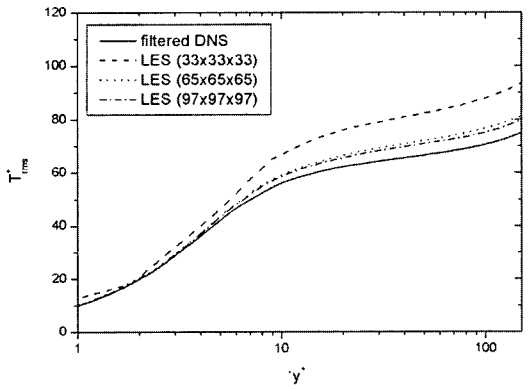

(a) mean scalar

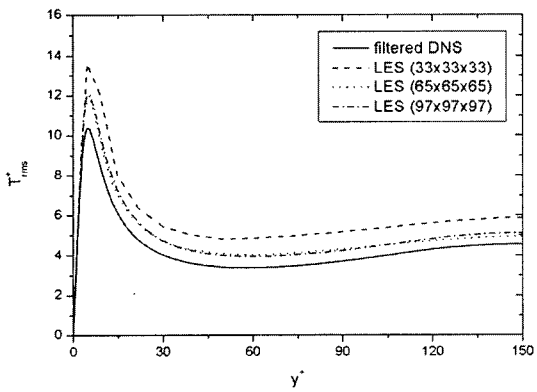

(b) rms scalar fluctuations

Fig. 2 Mean and rms scalar (temperature) profiles obtained from the LES with DMM for Pr=10 using three different resolutions

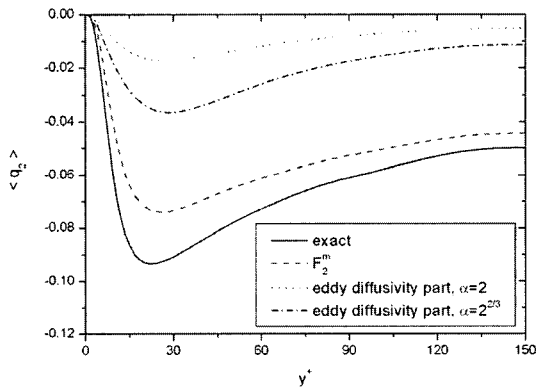

(a) Vertical SGS scalar flux

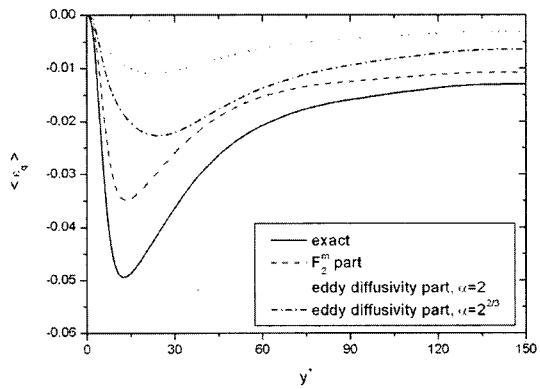

(b) SGS scalar dissipation

Fig. 3 Plane-averaged sub-grid scale scalar flux $\langle q_2 \rangle$ and scalar dissipation $\langle \varepsilon_q \rangle$ for Pr=1

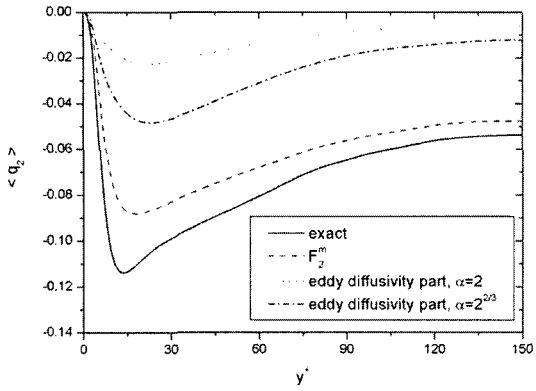

(a) Vertical SGS scalar flux

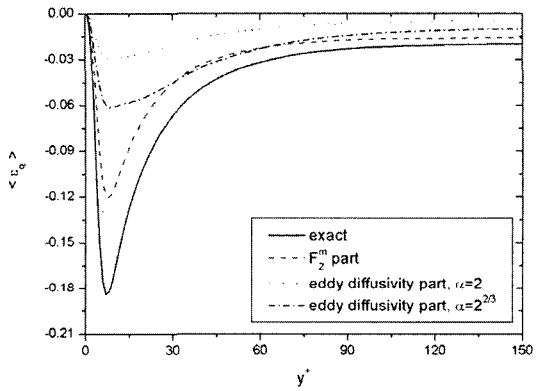

(b) SGS scalar dissipation

Fig. 4 Plane-averaged sub-grid scale scalar flux $\langle q_2 \rangle$ and scalar dissipation $\langle \varepsilon_q \rangle$ for Pr=3

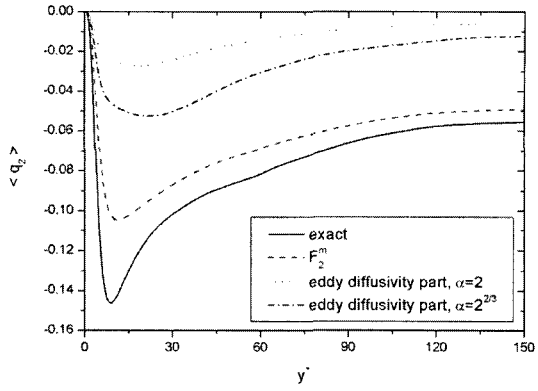

(a) Vertical SGS scalar flux

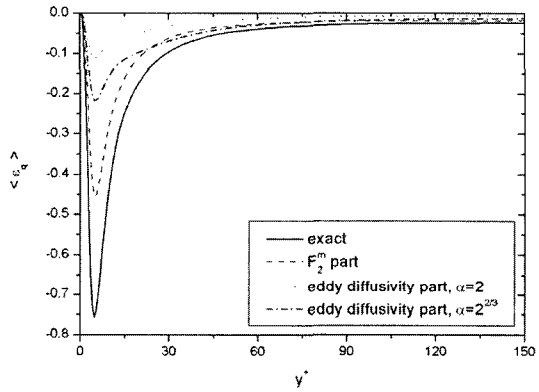

(b) SGS scalar dissipation

Fig. 5 Plane-averaged sub-grid scale scalar flux $\langle q_2 \rangle$ and scalar dissipation $\langle \varepsilon_q \rangle$ for Pr=10

flux $\langle q_2 \rangle$ and scalar dissipation $\langle \varepsilon_q \rangle$ for three different Prandtl numbers. It is seen that the magnitude of the eddy diffusivity part is significantly reduced by employing the mixed model for all the Prandtl numbers. So the too heavy burden placed on the model coefficient C_T by the DSM is effectively reduced, and this in turn will alleviate the need for ad hoc treatment to avoid numerical instability, such as spatial averaging of the model coefficients. Figures 3-5 suggest that the model's performance depends on the definition of the filter width ratio and $\alpha=2$ is generally better than $\alpha=2^{2/3}$ in reproducing the exact values of $\langle q_2 \rangle$ and $\langle \varepsilon_q \rangle$ obtained from the filtered DNS.

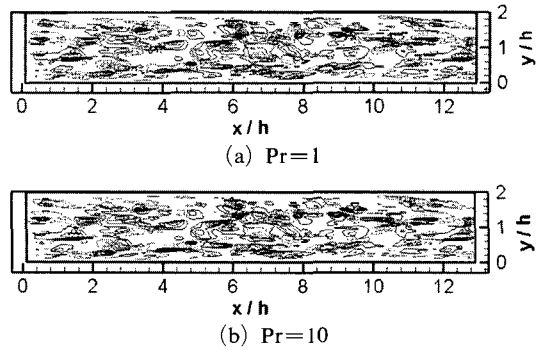

(a) Pr=1

(b) Pr=10

Fig. 6 Contours of model coefficient in the mid-plane of the domain. Contour levels are from −0.6 to 1.5 with an increment of 0.14

Contours of C_T in the mid-plane of the computational domain are plotted in Figure 6 for Pr=1 and 10. The contour values are from −0.6 to 1.5, with an increment of 0.14. In both cases, the regions of large value of C_T (corresponding to the regions with concentrated contours) are distributed in the channel for both Prandtl numbers considered. Negative C_T indicating SGS

backscatter also appears in many regions, but their magnitudes are much lower compared with the positive C_T in general. The correlation between C_S (not shown here) and C_T is not high except in the near-wall region, as can be deduced from the data of $Pr_{t,SGS}$ which will be discussed further in Figure 9.

The limiting behavior of α_t obtained with $\alpha=2$ for Pr=10 is shown in Figure 7. The expected behavior of α_t which varies with y^{+3} in the vicinity of the wall is evident. The α_t has rms levels always larger than the mean values throughout the channel. The ratio of the rms to the mean value of α_t varies from about 4~5 in the vicinity of the wall to 1.7 in the middle of the channel, indicating that α_t has more spikes in the region close to the wall. As mentioned earlier, by calculating the resolved term (F_j^m) explicitly in DMM, the eddy diffusivity part is significantly reduced and, as a result, the mean value of α_t turned out to be about 30% and 70% of the values obtained with the DSM near $y^+\approx 5$ and 60 respectively.

In Figure 8, contours of instantaneous vertical residual scalar flux vector q_2 are shown for Pr=10. Exact values of q_2 were directly calculated from the filtered DNS. The eddy diffusivity part $(-\alpha_t \partial\overline{T}/\partial x_j)$ and the resolved part (F_2^m) from the equation (13) were obtained from an a priori test. Note that similarity exists for the exact and the resolved parts of the scalar flux. This similarity means that the resolved part of the equation (13) provides a major part of the scalar flux vector and it alone can represent the local dynamics for the subgrid-scale scalar field rather successfully. Having a limited role of the modeled eddy diffusivity part supports Zang et al.'s (1993) claim that DMM requires less modeling through the explicit calculation of the modified Leonard term and the requirement to model only the residual stress even in the case of passive scalar.

The subgrid-scale turbulent Prandtl number, $Pr_{t,SGS}$ from the a priori test for Pr=1 and 10 is shown in Figure 9. The results from the actual LES with DMM and DSM are also included for comparison. The values of $Pr_{t,SGS}$ are lower by a factor of about 2 than the full-field turbulent Prandtl number in the middle of the channel, suggesting that the ratio of the eddy viscosity to eddy diffusivity changes with the spatial scales of the flow. This would suggest that the $Pr_{t,SGS}$ can depend on the molecular Prandtl number since the velocity and scalar fields have a different range of length scales depending on the molecular Prandtl number. In the present work, the same filter widths are used for both velocity and scalar fields by assuming that velocity and scalar fields will have a similar range of length scales, but

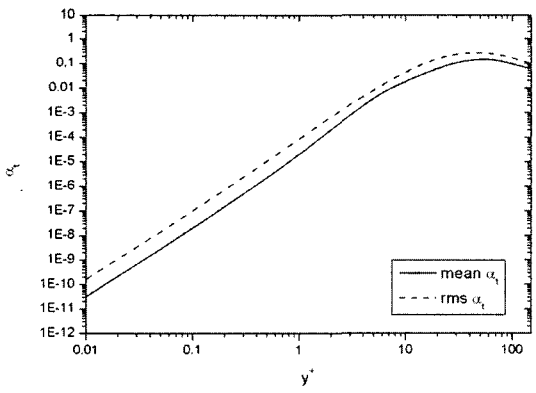

Fig. 7 Profiles of mean and rms SGS eddy diffusivity for Pr=10

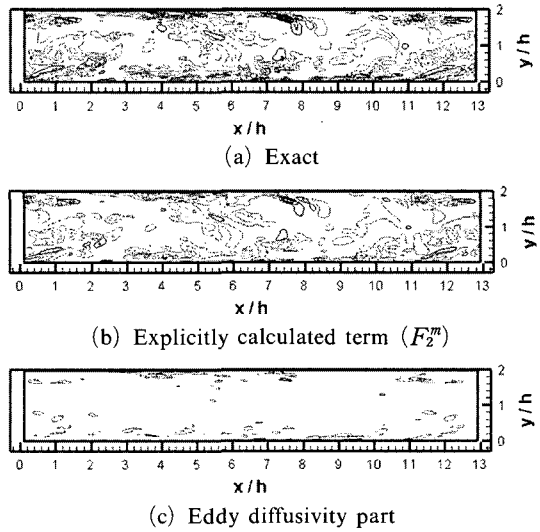

(a) Exact

(b) Explicitly calculated term (F_2^m)

(c) Eddy diffusivity part

Fig. 8 Contours of vertical residual heat flux vector in the middle of the domain for Pr=10. Contour levels are from -1.0 to 0.8 with an increment of 0.072

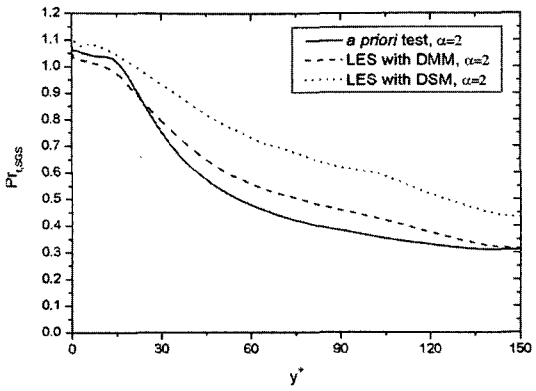

(a) Pr=1

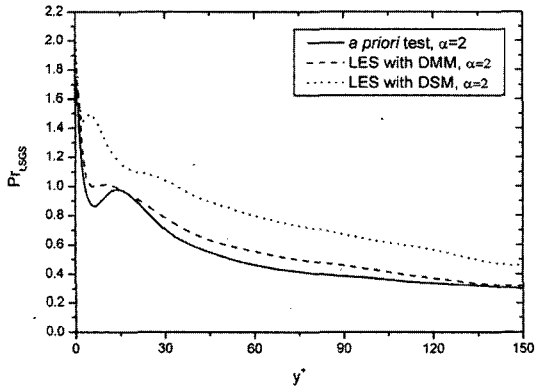

(b) Pr=10

Fig. 9 Turbulent Prandtl number at the subgrid-scale level

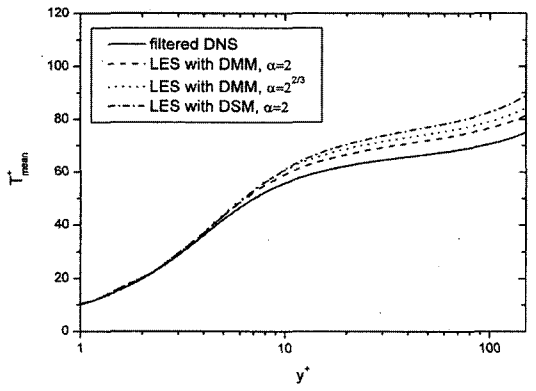

(a) mean scalar

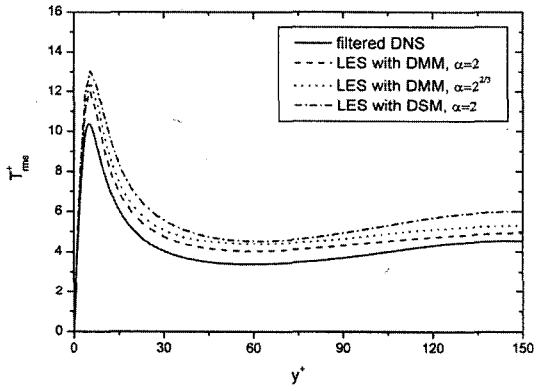

(b) rms scalar fluctuations

Fig. 10 Comparison of mean and rms scalar (temperature) profiles obtained from DNS and LES for Pr=10

apparently a judicious choice of filter width for the scalar field will be required for the high Prandtl number flows. It was found that $Pr_{t,SGS}$ was rather insensitive to the definition of filter width even though $\langle \tau_{12} \rangle$ and $\langle q_2 \rangle$ was influenced by α (Na, 2004), as clearly indicated in Figures (3)~(5). This is probably because $\langle \tau_{12} \rangle$ and $\langle q_2 \rangle$ are affected by α, but they change in a similar way so that the ratio of the eddy viscosity to eddy diffusivity remains unchanged. Figure 9 tells that DMM shows a better representation of subgrid-scale scalar field than DSM throughout the channel.

3.2 Results from LES

In order to determine the accuracy of the DMM for scalar transport, it was also tested a posteriori in the LES of a fully developed channel flow for Pr=10. Equations (13)~(19) were implemented in an LES code and the computations were performed with the same flow conditions as in the a priori tests. For comparison purposes, an LES with DSM using the same grid resolution was also carried out.

Figure 10 shows that all the mean scalar profiles obtained from the actual LES are higher in the log layer than in the DNS result. An inadequate resolution of the wall layer results in a low value of friction velocity that is reflected in a high value of the LES results in the logarithmic layer. Scalar intensities T^+_{rms} from LES (which do not include the unknown SGS components) are also compared with the filtered DNS in Figure 10. Again, all the LES results are consistently larger than the DNS, regardless of the values of α, due to the underestimated friction velocity. In general, DMM performs bet-

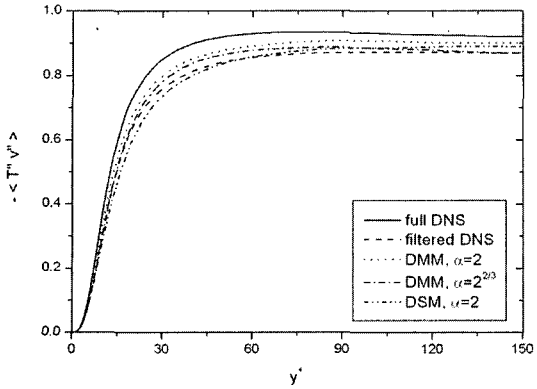

(a) Pr=1

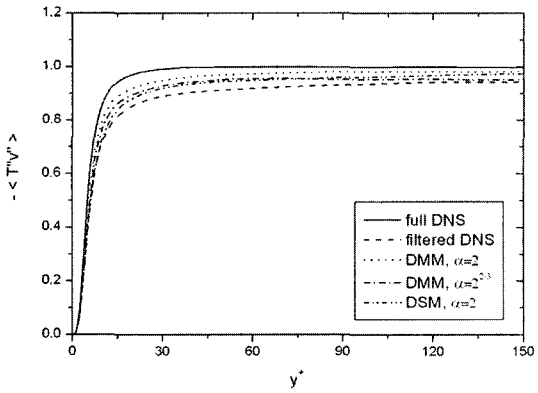

(b) Pr=10

Fig. 11 Correlation between resolved passive scalar and wall-normal velocity, $-\langle T''v''\rangle$

ter than DSM in the prediction of both T^+_{mean} and T^+_{rms}. The position of local peak values of T^+_{rms} in the near-wall region occurs near $y^+\approx 4.8$ for the filtered DNS and at about $y^+\approx 5.5$ for DMM with $\alpha=2$. A similar value of $y^+\approx 5.5$ was predicted for both DMM with and DSM with $\alpha=2$. Considering the resolution of the present LES in the vertical direction, it can be said that the local maximum location for T^+_{rms} is predicted reasonably with the LES.

Scalar fluxes $\langle T''v''\rangle$ (where $T''=\overline{T}-\langle\overline{T}\rangle$ and $v''=\overline{v}-\langle\overline{v}\rangle$) are plotted for Pr=1 and 10 in Figure 11. They are large-scale quantities resolved by the grid. For the normal component of scalar flux, improvement by DMM is not evident. It can be said from the figure that the correlations between the passive scalar and the wall-normal velocity were significantly underestimated by all the LES models which were tested here considering the fact that they consistently overpredicted the DNS data as shown in many other figures. The reason may be related to the fact that the wall normal velocity has a different range of length scale from those of streamwise velocity and passive scalar at the given Reynolds and Prandtl numbers as indicated in Na and Hanratty (2000), but obviously more work will be required to explain the behavior seen in Figure 11. If compared with SGS heat flux shown in Figures 3~5, it is noticed that contribution from the scale-similarity part $\langle F_j^m\rangle$ of residual scalar flux vector is an order of magnitude that is smaller than the large-scale turbulent heat flux $\langle T''v''\rangle$, except in the vicinity of the wall.

4. Summary

The dynamic mixed model of Zang et al. (1993) has been extended to the prediction of passive scalar transport with Prandtl number up to 10 in a turbulent channel flow. To assess the feasibility of the DMM applied to a passive scalar for high Prandtl number, a priori tests were carried out to determine the accuracy with which the model predicts both SGS scalar flux and dissipation.

An a priori test using DNS data indicates that the eddy diffusivity model performs successfully in the prediction of both SGS scalar flux and dissipation with $\alpha=2$. The explicitly calculated resolved terms constitute a major contribution to q_2, leaving the magnitude of the dynamically computed model coefficient C_T significantly reduced compared with that from DSM for all the Prandtl numbers considered.

Generalized DMM for scalar transport was also tested a posteriori in the LES of a fully developed channel flow for Pr=10. LES with DMM generally yields a better result than with DSM. A close investigation of the results suggests that the performance of the model showed little sensitivity to the size of the effective filter width ratio, as opposed to the result from the a priori test. Overall, the value of $\alpha=2$ produced a better result for the flow under investigation. If this optimal value for α varies considerably from

one flow to another, the applicability of the model will be reduced. Thus, more work will be required for a variety of complex, high Reynolds and Prandtl number flows in order to investigate the model's range of utility in its current form.

Acknowledgments

This paper was supported by Konkuk University in 2000.

References

Bardina, J., Ferziger, J. H. and Reynolds, W. C., 1983, "Improved Turbulence Models Based on Large Eddy Simulation of Homogeneous, Incompressible, Turbulent Flows," *Ph. D. dissertation, Dept. of Mechanical Engineering*, Stanford University.

Calmet, I. and Magnaudet, J., 1997, "Large-eddy Simulation of High-Schmidt Number Mass Transfer in a Turbulent Channel," *Phys. Fluids 9*, Vol. 2, pp. 438~455.

Germano, M., Piomelli, U., Moin, P. and Cabot, W. H., 1991, "A Dynamic Subgris-scale Eddy Viscosity Model," *Phys. Fluids, A 3*, Vol. 7, pp. 1760~1765.

Leonard, B. P., 1979, "A Stable and Accurate Convective Modeling Procedure Based on Quadratic Upstream Interpolation," *Comput. Methods Appl. Mech. Eng.*, Vol. 19, pp. 59~98.

Kang, S., 2000, "On Subgrid-Scale Models for Large Eddy Simulation of Turbulent Flows," *Transactions of the KSME (B)*, Vol. 24, No. 11, pp. 1523~1534.

Lilly, D.K., 1992, "A Proposed Modification of the Germano Subgrid-scale Closure Method," *Phys. Fluids, A 4*, pp. 633~635.

Na, Y., Papavassiliou, D. V. and Hanratty, T. J., 1999, "Use of Direct Numerical Simulation to Study the Effect of Prandtl Number on Temperature Fields," *Int. J. Heat Fluid Flow*, Vol. 20, pp. 187~195.

Na, Y. and Hanratty, T. J., 2000, "Limiting Behavior of Turbulent Scalar Transport Close to a Wall," *Int. J. Heat Mass Transfer*, Vol. 43, pp. 1749~1758.

Na, Y, 2004, "On the Large Eddy Simulation of High Prandtl Number Scalar Transport Using Dynamic Subgrid-Scale Model," *KSME Int. J.*, Vol. 18, No. 1, pp. 173~182.

Zang, W., Street, R. L. and Koseff, J. R., 1993, "A Dynamic Mixed Subgrid-scale Model and its Application to Turbulent Recirculating Flows," *Phys. Fluids, A 5*, Vol. 12, pp. 3186~3196.